

Density Functional Theory Studies of the Magnetostructural Correlations in the Cyano-Bridged Mo₂Ni and Mo₂Ni₃ Systems

Yi-Quan Zhang*^[a] and Cheng-Lin Luo^[a]

Keywords: Molecular magnetism / Density functional calculations / Broken symmetry / Cyano-bridged systems / Molybdenum

A theoretical density functional study of the magnetostructural correlations in a series of cyano-bridged MoNi systems is presented. Our calculations by two approaches with several local density approximations (LDAs) and generalized gradient approximations (GGAs) show that: (1) the influence of the next-nearest-neighbor MoMo interactions on the MoNi interactions can be omitted; (2) the MoNi interactions strengthen with an increase in the Ni–N_{brid}–C_{brid} angle in the range 135° to 175° for all the functionals; (3) increasing the number of exchange coupling interactions from one to two

will decrease the ferromagnetic MoNi interactions, but the influence of further increasing the number of exchange coupling interactions from two to three or four on the MoNi interactions is very small, because the peripheral units do not surround the same central metal ion in the MoNi systems that we investigated. Kahn's theory was used to interpret the above results.

(© Wiley-VCH Verlag GmbH & Co. KGaA, 69451 Weinheim, Germany, 2008)

Introduction

In recent years, the synthesis and study of polynuclear molecules having high-total-spin ground states and anisotropy has received much attention.^[1–4] These anisotropic high-spin molecules exhibit original magnetic properties such as single molecule magnet (SMM) behavior^[1] or the magnetic quantum tunneling effect.^[2] In these molecule magnets, much attention has been focused on developing cyano-bridged cluster systems, for which the ground state spin value *S* and the zero-field splitting parameter *D* are more readily adjusted by substitution of various metal ions.^[3–4] However, in these cyano-bridged systems, a lot of problems, such as the relationships between the exchange coupling constants *J* and the bridging angles and the number of exchange interactions and the parameter *D*, puzzle us. Thus, the studies of the cyano-bridged cluster systems are important for us to search novel molecular magnetic materials with higher blocking temperatures.

Long and co-workers^[5] considered that attaching two Ni^{II} centers to the [(Me₃tacn)Mo(CN)₃] (Me₃tacn = *N,N',N''*-trimethyl-1,4,7-triazacyclononane) unit in the complex [(Me₃tacn)₂(cyclam)₃(H₂O)₂Ni₃Mo₂(CN)₆]⁶⁺ (cyclam = 1,4,8,11-tetraazacyclotetradecane) (**13** in ref.^[5]) can cause a substantial reduction in the strength of the magnetic coupling, and the smaller coupling constant relative to that of the complex [α-(Me₃tacn)₂(cyclam)NiMo₂(CN)₆]²⁺ (**8** in ref.^[5]) is associated with the central Ni^{II},

which is involved in the exchange interactions with two Mo^{III} centers rather than just one. As we know, magnetic exchange coupling interactions are associated to several structural factors, such as bond lengths and bridging angles. In the above-mentioned complexes **8** and **13** in ref.^[5], the bridging bond lengths and the Mo–C_{brid}–N_{brid} angles are almost the same, but the bridging Ni–N_{brid}–C_{brid} angles are very different. Hence, we know that the two important structural factors, the bridging Ni–N_{brid}–C_{brid} angle and the number of peripheral complexes, both influence the MoNi interactions. To investigate the relationships between the MoNi interactions and the bridging Ni–N_{brid}–C_{brid} angles and the number of peripheral complexes, we selected the complexes [(Me₃tacn)₂(cyclam)₃(H₂O)₂Ni₃Mo₂(CN)₆]⁶⁺ and [α-(Me₃tacn)₂(cyclam)NiMo₂(CN)₆]²⁺.^[5] Finally, Kahn's qualitative theory^[6–7] was used to interpret the calculated results.

Description of the Complexes and Models

Complex A, [α-(Me₃tacn)₂(cyclam)NiMo₂(CN)₆]²⁺ (see Figure 1),^[5] contains two MoNi units taking part in exchange interactions.

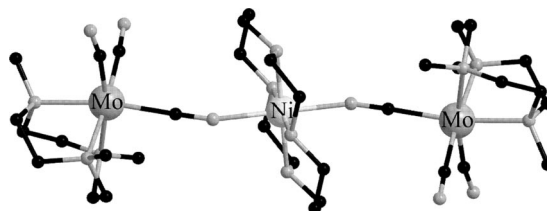
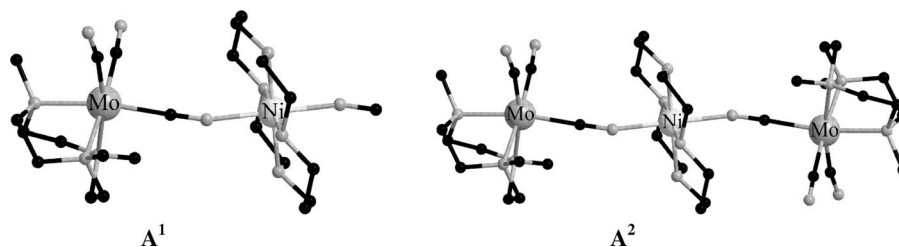
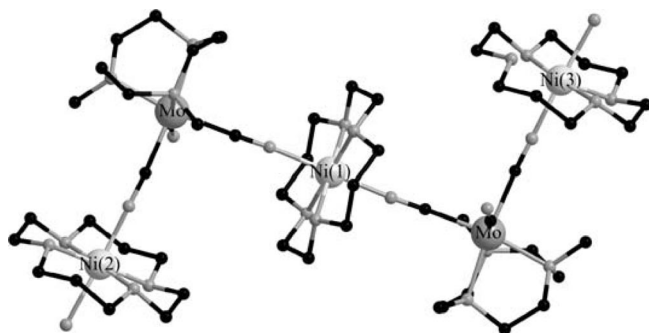


Figure 1. Structure of complex A (Mo₂Ni).

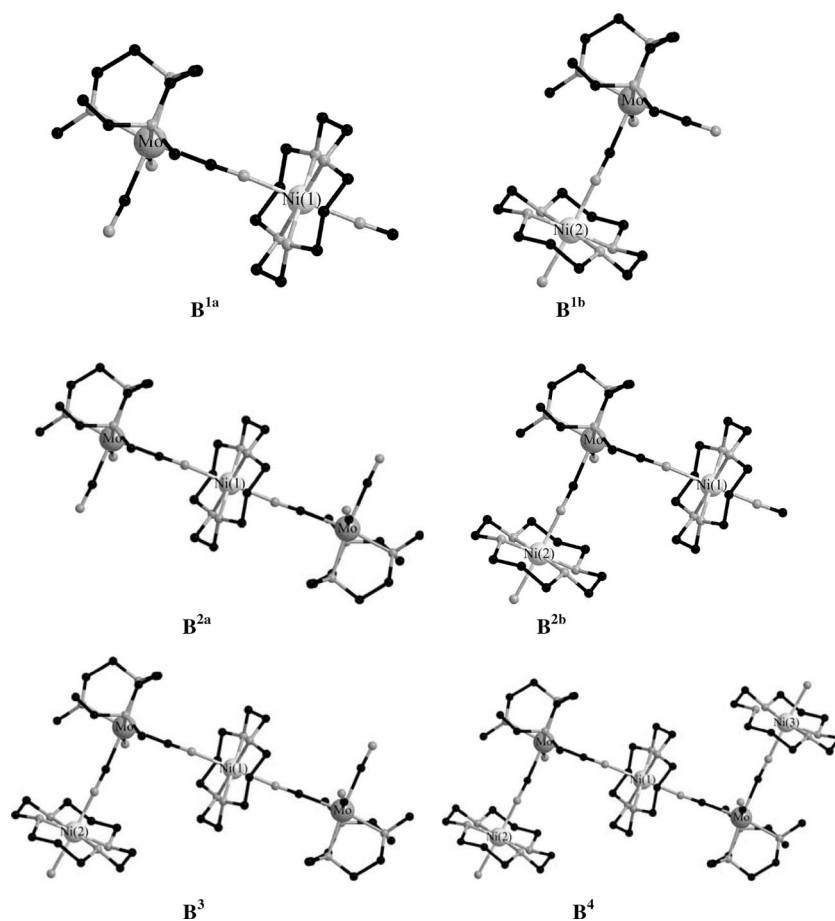
[a] School of Physical Science and Technology, Nanjing Normal University, Nanjing 210097, China
E-mail: zhangyiquan@njnu.edu.cn

Figure 2. Structures of models A^1 (left) and A^2 (right).Figure 3. Structure of complex **B**.

Two CN ligands bridge the nickel ion. The $\text{Ni-N}_{\text{brid}}-\text{C}_{\text{brid}}$ angles deviate moderately from linearity ($\text{Ni-N}_{\text{brid}}-\text{C}_{\text{brid}} = 163.57^\circ$). Models A^1 and A^2 (the superscripted numbers denote the number of peripheral complexes; see Figure 2) are the modeled structures of complex **A**.

Complex **B**, $[(\text{Me}_3\text{tacn})_2(\text{cyclam})_3(\text{H}_2\text{O})_2\text{Ni}_3\text{Mo}_2(\text{CN})_6]^{6+}$ (see Figure 3),^[5] contains four MoNi units participating in exchange interactions.

The $\text{Ni}(1)-\text{N}_{\text{brid}}-\text{C}_{\text{brid}}$ angles are both 175.12° . The $\text{Ni}(2)-\text{N}_{\text{brid}}-\text{C}_{\text{brid}}$ and $\text{Ni}(3)-\text{N}_{\text{brid}}-\text{C}_{\text{brid}}$ angles are both 170.81° . Models B^{1a} , B^{1b} , B^{2a} , B^{2b} , B^3 , and B^4 (the superscripted numbers denote the number of MoNi units; **a** and **b** denote the different MoNi units; see Figure 4) are the modeled structures of complex **B**.

Figure 4. Structures of models B^{1a} , B^{1b} , B^{2a} , B^{2b} , B^3 , and B^4 .

In all figures, H atoms are omitted. All the models were directly taken from complexes **A** and **B**, and they were not optimized, because small changes to the experimental structures could result in significant deviations for the coupling constants.

Results and Discussion

Evaluation of J for Each Model

The details of the computations can be found in the Computational Details section at the end of this manuscript. The J values for models **A**¹, **A**², **B**^{1a}, **B**^{1b}, **B**^{2a}, **B**^{2b}, **B**³, and **B**⁴, which were calculated by using two approaches with several LDAs and GGAs, and the experimental values are shown in Table 1.^[5]

Table 1. Experimental and calculated J and J' values [cm⁻¹] for models **A**¹, **A**², **B**^{1a}, **B**^{1b}, **B**^{2a}, **B**^{2b}, **B**³, and **B**⁴. In the calculations, two approaches were used ("First" and "Second" represent the first BS approach and the second approach, respectively.) with several functionals in the Amsterdam Density Functional (ADF).

	Approach	VWN	PW91	PBE	OPerdew	OPBE	Exp.	
A ¹	J First (MoNi)	41.8	30.1	31.6	43.9	43.9		
A ²	J First (MoNiY)	27.9	22.0	22.6	30.0	29.8	17.6 ^[5]	
	Second (Mo ₂ Ni)	24.6	19.2	19.8	26.2	26.0		
	J_{MoMo} First (MoMoZn)	0.01	0.01	0.01	0.01	0.01		
B ^{1a}	J First (MoNi)	65.1	46.6	48.3	57.5	57.9		
B ^{1b}	J' First (MoNi)	35.7	27.4	28.2	35.1	34.9		
B ^{2a}	J First (MoNiY)	37.0	29.4	30.1	36.7	36.6		
	Second (Mo ₂ Ni)	32.6	25.8	26.4	32.1	31.9		
B ^{2b}	J' First (MoNiY)	27.3	19.5	20.1	27.0	26.6		
	Second (Mo ₂ Ni)	23.5	16.3	16.8	23.4	23.1		
B ³	J First (MoNiYZn)	37.6	30.0	31.1	37.2	37.0		
	Second (Mo ₂ Ni ₂)	31.4	24.9	25.2	31.0	30.8		
	J'	First (MoNiYZn)	27.8	20.1	20.9	27.1	26.5	
		Second (Mo ₂ Ni ₂)	23.9	16.8	17.2	23.4	23.1	
B ⁴	J First (MoNiYZn ₂)	40.8	31.9	32.6	39.5	39.4	4.0 ^[5]	
	Second (Mo ₂ Ni ₃)	30.7	24.3	25.0	30.9	31.0		
	J'	First (MoNiYZn ₂)	28.0	21.1	21.6	27.4	27.3	8.5 ^[5]
Second (Mo ₂ Ni ₃)		24.2	17.3	17.8	23.7	23.5		

For all the models, the J values calculated by using PW91 are the ones closest to the experimental values.^[5] The GGAs OPerdew and OPBE give the poorer J values for MoNi systems in which the interactions are ferromagnetic, although they give the relatively better J values for CrMn and MoMn systems in which the interactions are antiferromagnetic.^[8,9] For all the models, the second approach with all the functionals gives the better J values relative to those obtained with the broken symmetry (BS) approach, as found in our previous papers.^[8–11] To our surprise, however, the calculated J values for model **A**² are close to the experimental one, but the calculated J and J' values for models **B**³ and **B**⁴ have larger differences from the experimental values. In the next sections, we will interpret the reasons for these observations.

Comparison and Analysis of the Exchange Interactions in Models **A**¹, **A**², **B**^{1a}, **B**^{1b}, **B**^{2a}, **B**^{2b}, **B**³, and **B**⁴

The J values for **A**¹ and **A**², calculated by using all the functionals, show that the MoNi ferromagnetic interactions decrease with an increase in the number of exchange interactions. As we know, the next-nearest neighbor MoMo antiferromagnetic interactions in **A**² might decrease the MoNi interactions. In ref.^[5], the authors concluded that including the next-nearest neighbors to account for long-range coupling between the two Mo centers did not improve the fit and did not reproduce the drop in $\chi_{\text{M}}T$ at lower temperatures from the experimental data. In addition, the influence of the next-nearest neighbor on MoNi interactions is very small (the MoMo exchange coupling constants J_{MoMo} of **A**², calculated by using the BS approach with several functionals, are all very small; see Table 1). Therefore, we conclude that the decrease in the J values from **A**¹ to **A**² is mainly due to the increase in the number of exchange interactions.

From Table 1, the calculated J values for **B**^{1a} are larger than the J' values for **B**^{1b}. This can be rationalized by looking at the structures of the above models. An important structural difference between models **B**^{1a} and **B**^{1b}, which influences the MoNi interactions, is the Ni–N_{brid}–C_{brid} angle. Its value is greater for **B**^{1a} (175.12°) than for **B**^{1b} (170.81°). Marvaud and co-workers^[4] concluded, from experimental results, that the ferromagnetic interactions between Cr^{III} and Ni^{II} in the cyano-bridged CrNi complexes increase with increasing Ni–N_{brid}–C_{brid} angle. In our previous paper,^[10] we also presented the same conclusion by using the BS approach. In order to determine whether MoNi interactions increase with increasing Ni–N_{brid}–C_{brid} angle for MoNi systems as well, we calculated the J values for **A**¹ (its structure is similar to those of **B**^{1a} and **B**^{1b}) for a range of Ni–N_{brid}–C_{brid} angles between 135° and 180°. The plot of J versus Ni–N_{brid}–C_{brid} angle (Figure 5) shows that J values increase with an increase in the Ni–N_{brid}–C_{brid} angle in the range 135° to 175° with all the functionals.

The lines connecting the data points in Figure 5, and also those in the next figure, were all fitted by the Gaussian function. Other functions can also be used to fit the lines. However, our main aim is to clearly find the variation of these data points from the fitted lines irrespective of the function that is to be used. The above results can be simply rationalized by Kahn's theory,^[6–7] which states that the increase in the Ni–N_{brid}–C_{brid} angle will lead to a decrease in the overlap integral and therefore to an increase in the ferromagnetic coupling constants J . A thorough discussion of the relationship between the J and the overlap integral will be given in the next section. However, as the Ni–N_{brid}–C_{brid} angle increases from 175° to 180°, the J values decrease. This might be due to the amount of antiferromagnetic interaction that is probably overestimated, since the complex was not re-optimized by holding the bond angle fixed. From the above calculations, we understand why the calculated J values for **B**^{1a} (Ni–N_{brid}–C_{brid} = 175.12°) are larger than those for **B**^{1b} (Ni–N_{brid}–C_{brid} = 170.81°).

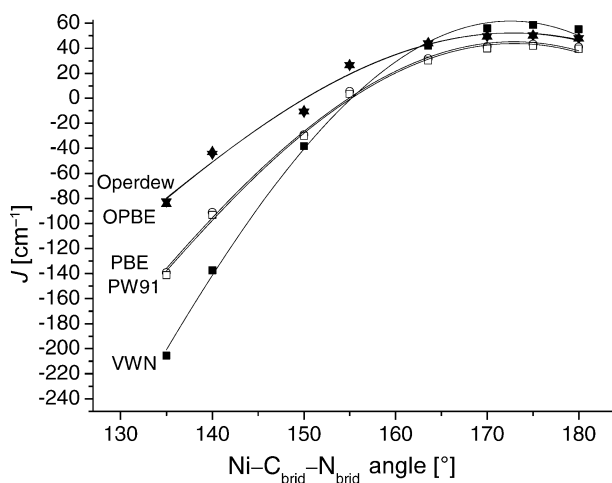


Figure 5. Dependence of the exchange coupling constants J of \mathbf{A}^1 on the $\text{Ni-N}_{\text{brid}}\text{-C}_{\text{brid}}$ angle in the range $135\text{--}180^\circ$. The J values were calculated with several functionals [VWN (\blacksquare), PW91 (\square), PBE (\circ), OPBE (\blacktriangledown), and Operdew (\blacklozenge)] by using the BS approach.

From the calculated J values for \mathbf{B}^{1a} and \mathbf{B}^{2a} , we find that the J values decrease with an increase in the number of exchange interactions from \mathbf{B}^{1a} to \mathbf{B}^{2a} . However, the decrease in J' is small from \mathbf{B}^{1b} to \mathbf{B}^{2b} . The above results show that attaching another $[(\text{Me}_3\text{tacn})\text{Mo}(\text{CN})_3]$ to $[(\text{cyclam})\text{Ni}]$ will decrease the MoNi ferromagnetic interactions, but the influence of attaching another $[(\text{cyclam})\text{Ni}]$ to $[(\text{Me}_3\text{tacn})\text{Mo}(\text{CN})_3]$ on the MoNi interactions is small. Our previous paper^[9] shows that larger MoMnMo angles have a larger influence on the MoMn interactions. For models \mathbf{B}^{2a} and \mathbf{B}^{2b} , the MoNiMo angle in \mathbf{B}^{2a} and the NiMoNi angle in \mathbf{B}^{2b} are 180° and 94.6° , respectively. The larger MoNiMo angle has a larger influence on the MoNi interactions in \mathbf{B}^{2a} than that of the smaller NiMoNi angle in \mathbf{B}^{2b} . Therefore, we find that the decrease in J from \mathbf{B}^{1a} to \mathbf{B}^{2a} is larger than that from \mathbf{B}^{1b} to \mathbf{B}^{2b} .

The calculated J values for \mathbf{B}^{2a} , \mathbf{B}^3 , and \mathbf{B}^4 are almost the same, which can be understood from the above results that the influence of attaching another $[(\text{cyclam})\text{Ni}]$ to $[(\text{Me}_3\text{tacn})\text{Mo}(\text{CN})_3]$ on the MoNi interactions is small. However, we also find that the J' value for \mathbf{B}^{2b} , \mathbf{B}^3 , and \mathbf{B}^4 are almost the same, which shows that the next-nearest units have a small influence on the MoNi interactions. In our previous papers,^[8–10] we found that the magnetic coupling interactions weaken with an increase in the number of exchange interactions, regardless of whether the interactions are ferromagnetic or antiferromagnetic, for a series of complexes. However, why are the variations of the MoNi interactions very small from \mathbf{B}^{2a} to \mathbf{B}^4 or \mathbf{B}^{2b} to \mathbf{B}^4 ? This can be explained by the differences in their structures. As indicated above, the nearest units influence the MoNi interactions, but the next-nearest units have a small influence. Thus, the interactions in our previously investigated complexes, in which the peripheral units all surround one center, will decrease with an increase in the number of exchange interactions, but they are almost the same from \mathbf{B}^{2a} to \mathbf{B}^4 or from \mathbf{B}^{2b} to \mathbf{B}^4 , because they do not surround the same

central metal ion for \mathbf{B}^3 and \mathbf{B}^4 . Kahn's qualitative theory^[6–7] will be used to interpret the reason in the next sections. The J and J' values compared were calculated by using the same approach and functional.

The $\text{Ni-N}_{\text{brid}}\text{-C}_{\text{brid}}$ angles of \mathbf{A}^2 and \mathbf{B}^{2a} are 163.57° and 175.12° , respectively. From Figure 5, we know that the J values increase with an increase in the $\text{Ni-N}_{\text{brid}}\text{-C}_{\text{brid}}$ angles. As we expected, the calculated J values for \mathbf{B}^{2a} are larger than those for \mathbf{A}^2 (Table 1). However, the experimental J value for \mathbf{B}^4 (4.0 cm^{-1}) is much smaller than that for \mathbf{A}^2 (17.6 cm^{-1}). As the above results indicated, the differences in the calculated J values for \mathbf{B}^{2a} and \mathbf{B}^4 are small, and therefore, the J value for \mathbf{B}^4 should be larger than that for \mathbf{A}^2 . Moreover, we find that the experimental J value for compound $\mathbf{14}$ in ref.^[5] (for which the $\text{Ni-N}_{\text{brid}}\text{-C}_{\text{brid}}$ angle is about 171°), which has a similar structure to that of \mathbf{B}^4 , is 14.9 cm^{-1} , which is much larger than that for \mathbf{B}^4 . Therefore, we consider that the experimental J value for \mathbf{B}^4 may have been underestimated by Long and co-workers. For the same reason, the experimental J' value for \mathbf{B}^4 may also have been underestimated by them.

The following conclusions can be extracted from the results of our calculations on MoNi systems: (1) the influence of the next-nearest neighbor MoMo interactions on the MoNi interactions can be omitted, thus, the decrease in the J values from \mathbf{A}^1 to \mathbf{A}^2 is mainly due to the increase in the number of exchange interactions; (2) the J values increase with an increase in the $\text{Ni-N}_{\text{brid}}\text{-C}_{\text{brid}}$ angle in the range $135\text{--}175^\circ$ with all the functionals; (3) attaching a $[(\text{Me}_3\text{tacn})\text{Mo}(\text{CN})_3]$ moiety to $[(\text{cyclam})\text{Ni}]$ will decrease the MoNi ferromagnetic interactions, but the influence of attaching a $[(\text{cyclam})\text{Ni}]$ moiety to $[(\text{Me}_3\text{tacn})\text{Mo}(\text{CN})_3]$ on the MoNi interactions is small for the smaller NiMoNi angle from the calculated J and J' values for \mathbf{B}^{1a} , \mathbf{B}^{2a} , \mathbf{B}^{1b} , and \mathbf{B}^{2b} ; (4) the next-nearest units have a small influence on the MoNi interactions from the calculated J' for \mathbf{B}^{2b} , \mathbf{B}^3 , and \mathbf{B}^4 for their structures in which the peripheral units do not surround one magnetic center.

Qualitative Analysis of the Exchange Interaction

According to Kahn's theory,^[6–7] the exchange coupling constant, J_{ab} , is expressed by Equation (1).

$$J_{\text{ab}} \approx K_{\text{ab}} - S_{\text{ab}}(\Delta^2 - \delta^2)^{1/2} \quad (1)$$

The positive term, K_{ab} , represents the ferromagnetic contribution, J_{F} , favoring parallel alignment of the spins and a triplet ground state, while the negative term $-S_{\text{ab}}(\Delta^2 - \delta^2)^{1/2}$ is the antiferromagnetic contribution J_{AF} , favoring anti-parallel alignment of the spins and a singlet ground state. S_{ab} is the overlap integral between a and b. δ is the initial energy gap between the magnetic orbitals, Δ is the energy gap between the molecular orbitals derived from them. When several electrons are present on each center, n_x on one site, n_y on the other, J can be described by the sum of the different "orbital pathways", J_{ab} , defined as above for pairs of orbitals a and b located on each site, weighted by the number of electrons [see Equation (2)].

$$J = \sum_{a,b} J_{ab}/n_x \times n_y \quad (2)$$

Some authors^[12,13] have recently shown that magnetic orbitals a and b are well represented by the localized orbitals of the broken-symmetry solution (called BS-OMSO in ref.^[14]). There are six different contributions to the exchange coupling constant in each Mo^{III}Ni^{II} pair. The mean overlap integral, S_{ij} , between the six orbitals of Mo^{III} and Ni^{II} can be expressed in Equation (3).

$$S_{ij} = (d_{xy}d_{x^2-y^2} + d_{yz}d_{x^2-y^2} + d_{zx}d_{x^2-y^2} + d_{xy}d_{z^2} + d_{yz}d_{z^2} + d_{zx}d_{z^2})/6 \quad (3)$$

According to a recent study by E. Ruiz and co-workers,^[15] S_{ij}^2 can be correlated to Δ_{xy} [Equation (4)] for polynuclear complexes calculated by using the second approach.

$$\Delta_{xy} = [\sqrt{(\rho_{HS}^x)^2 - (\rho_{LS}^x)^2} + \sqrt{(\rho_{HS}^y)^2 - (\rho_{LS}^y)^2}]^2 \quad (4)$$

Here $\rho_{HS,LS}^{x,y}$ are the different spin populations of the paramagnetic centers x or y involved in the exchange interaction in the highest (HS) or lowest (LS) spin configurations. Equation (4) tells us that the values of $(\rho_{HS}^x)^2$ should be larger than those of $(\rho_{LS}^x)^2$. All the calculated values of $(\rho_{HS}^x)^2$ are larger than the calculated $(\rho_{LS}^x)^2$ values. Thus, Equation (4) can be used to interpret the magnetostructural correlations for polynuclear complexes calculated by using the second approach.

For binuclear models calculated by the BS approach, we find that the calculated $(\rho_{HS}^x)^2$ are not always larger than $(\rho_{BS}^x)^2$. We therefore used a revised Δ_{xy} , as indicated in Equation (5).

$$\Delta_{xy} = [\sqrt{(\rho_{HS}^x)^2 - (\rho_{BS}^x)^2} \pm \sqrt{(\rho_{HS}^y)^2 - (\rho_{BS}^y)^2}]^2 \quad (5)$$

If the signs of $(\rho_{HS}^x)^2 - (\rho_{BS}^x)^2$ and $(\rho_{HS}^y)^2 - (\rho_{BS}^y)^2$ are the same, we should use the plus sign in Equation (5). Otherwise, the minus sign should be adopted in Equation (5). The spin density populations on Mo^{III} and Ni^{II} were obtained with Mulliken Population Analysis^[16] calculated by using the PW91 functional. The strength of the S_{ij}^2 should be linearly dependent on Δ_{xy} [Equation (6)].

$$S_{ij}^2 \propto \Delta_{xy} \quad (6)$$

The relationship between J and Δ_{xy} for **A**¹, as its Ni–N_{brid}–C_{brid} angle changes from 135° to 180°, is shown in Figure 6. The J values, calculated by using the BS approach with the PW91 functional, increase with decreasing Δ_{xy} .

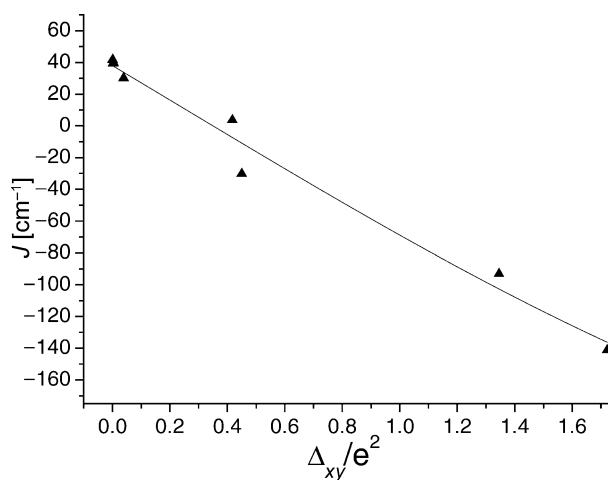


Figure 6. Dependence of the exchange coupling constants J for **A**¹ on Δ_{xy} as the Ni–N_{brid}–C_{brid} angle is varied from 135° to 180°. The J values were calculated with the PW91 functional by using the BS approach.

This result can be simply rationalized according to Equations (1) and (6) to conclude that the decrease in Δ_{xy} will reduce the antiferromagnetic contributions and then lead to an increase in the overall J value ($J = J_F + J_{AF}$).

Then, we calculated the Δ_{xy} for models **A**¹, **A**², **B**^{1a}, **B**^{1b}, **B**^{2a}, **B**^{2b}, **B**³, and **B**⁴ by using two approaches with the PW91 functional (see Table 2).

Analysis of the results in Table 2 shows that the calculated J or J' are all almost linearly dependent on the corresponding Δ_{xy} and that the MoNi interactions strengthen with decreasing Δ_{xy} , which shows that S_{ij}^2 can be correlated to Δ_{xy} in Equations (4) and (5) to interpret the magnetostructural correlations. The Δ_{xy} values for **A**², **B**^{2a}, and **B**^{2b} calculated by using the BS approach are larger than those of **A**¹, **B**^{1a}, and **B**^{1b}, respectively, which will result in a decrease in the calculated J or J' from **A**², **B**^{2a}, and **B**^{2b} to **A**¹, **B**^{1a}, and **B**^{1b} (Table 1), respectively, according to Equations (1) and (6). The above result shows that the increase in the number of exchange coupling interactions from one to two will decrease the ferromagnetic MoNi interactions. However, from the calculated Δ_{xy} values for **B**^{2a}, **B**³, and **B**⁴ (corresponding to J) or **B**^{2b}, **B**³, and **B**⁴ (corresponding to J'), the Δ_{xy} values calculated by using the same

Table 2. Calculated Δ_{xy} (e²) and J or J' values [cm⁻¹] for models **A**¹, **A**², **B**^{1a}, **B**^{1b}, **B**^{2a}, **B**^{2b}, **B**³, and **B**⁴ by the PW91 functional with two approaches (the First BS and the Second).

Type	A ¹	A ²	B ^{1a}	B ^{1b}	B ^{2a}	B ^{2b}	B ³	B ⁴								
Approach	J	J	J	J'	J	J'	J	J'	J	J'	J	J'	J	J'	J	J'
	First	First	First	First	First	Second	First	Second	First	Second	First	Second	First	Second	First	Second
Δ_{xy}	0.039	0.056	0.004	0.049	0.044	0.067	0.071	0.096	0.041	0.068	0.071	0.097	0.040	0.069	0.073	0.098
J or J'	30.1	22.0	46.6	27.4	29.4	25.8	19.5	16.3	30.0	24.9	20.1	16.8	31.9	24.3	21.1	17.3

approach are almost the same, which shows that increasing the number of exchange coupling interactions from two to three or four will not decrease the ferromagnetic MoNi interactions.

Conclusions

Two approaches with several LDAs and GGAs were used to investigate the magneto-correlations of the selected MoNi systems. From the calculations, we conclude that: (1) the influence of the next-nearest-neighbor MoMo interactions on the MoNi interactions can be omitted, thus, the decrease in the J values from \mathbf{A}^1 to \mathbf{A}^2 is mainly due to the increase in the number of exchange interactions; (2) from the calculated J values for \mathbf{A}^1 with varying Ni–N_{brid}–C_{brid} angle, we found that the J values increase with an increase in the Ni–N_{brid}–C_{brid} angle in the range 135–175° with all the functionals; (3) the next-nearest units have a small influence on the MoNi interactions as indicated by the calculated J' values for \mathbf{B}^{2b} , \mathbf{B}^3 , and \mathbf{B}^4 for their structures in which the peripheral units do not surround one magnetic center. The above results show that an increase in the number of exchange coupling interactions from one to two will decrease the ferromagnetic MoNi interactions, but the influence of increasing the number of exchange coupling interactions from two to three or four on the MoNi interactions is very small. Thus, we consider that the experimental J value for \mathbf{B}^4 may have been underestimated by Long and co-workers.^[5] Moreover, the experimental J value for compound **14** in ref.^[5] (the Ni–N_{brid}–C_{brid} is about 171°)^[5] having a similar structure to that of \mathbf{B}^4 is 14.9 cm⁻¹, which is much larger than that of \mathbf{B}^4 . This observation also confirms our conclusion. The results may be extended to other similar systems. For polynuclear models calculated by using the second approach, Equation (4) is appropriate for interpreting the magnetostructural correlations. However, for binuclear models calculated by using the BS approach, a revised Δ_{xy} [Equation (5)] proposed by us is more appropriate.

Computational Details

Two different approaches were used for calculating the exchange coupling constants for the polynuclear complexes.^[17–19] In all the calculations, the spin-orbit coupling was not considered, so taking into account the magnetic anisotropy was not necessary. The first approach consisted of evaluating the exchange coupling constant, J_{ij} , between two paramagnetic metal centers, i and j , in the hexanuclear molecule by calculating the energy difference between the highest and broken-symmetry spin states of a model molecule in which metal atoms except for the above-mentioned i and j are substituted by diamagnetic Zn^{II} for Ni^{II} and Y^{III} for Mo^{III}. This approach was used to calculate the exchange coupling interactions of hexanuclear complexes in many papers and proved to provide results that were in agreement with the experimental ones.^[17–20] The second approach is to calculate the different spin state energies of hexanuclear complexes and use the Heisenberg Hamiltonian to obtain the exchange coupling constants between different metal centers.^[17–21] This is the more rigorous approach with respect to the

first one in evaluating J for polynuclear complexes. The use of the two approaches will be discussed thoroughly below.

At first, we discuss the first approach. The magnetic interactions between Cr^{III} and Ni^{II} ions were studied on the basis of the density functional theory (DFT) coupled with the broken symmetry approach (BS).^[22–24] The exchange coupling constants, J , have been evaluated by calculating the energy difference between the high-spin state (E_{HS}) and the broken symmetry state (E_{BS}). Let us assume that the spin Hamiltonian is defined by Equation (7).

$$\hat{H} = -2J\hat{S}_1 \cdot \hat{S}_2 \quad (7)$$

If the spin-projected approach is used, the equation proposed by Noodleman^[22–24] to extract the J value for a binuclear transition-metal complex is given by Equation (8).

$$J = \frac{E_{\text{BS}} - E_{\text{HS}}}{4S_1S_2} \quad (8)$$

For all the models \mathbf{A}^1 , \mathbf{A}^2 , \mathbf{B}^{1a} , \mathbf{B}^{1b} , \mathbf{B}^{2a} , \mathbf{B}^{2b} , \mathbf{B}^3 , and \mathbf{B}^4 , where $S_1 = 3/2$ for Mo^{III}, $S_2 = 1$ for Ni^{II}, and from Equation (8), we get the expression in Equation (9).

$$J = (E_{\text{BS}} - E_{\text{HS}})/6 \quad (9)$$

Equations (8) and (9) are only used for binuclear compounds such as \mathbf{A}^1 , \mathbf{A}^2 , \mathbf{B}^{1a} , and \mathbf{B}^{1b} . In the calculations for polynuclear complexes such as \mathbf{B}^{2a} , \mathbf{B}^{2b} , \mathbf{B}^3 , and \mathbf{B}^4 , we used the diamagnetic Zn^{II} to replace the other Ni^{II} and Y^{III} to replace the other Mo^{III}; the resulting MoNiZn_{*n*}Y_{*m*} complex is equivalent to a binuclear MoNi complex from the magnetic point of view, and we can therefore use Equation (8) and (9) to obtain the exchange coupling constants, J .

According to recent reports by Ruiz et al. based on a number of calculations on the magnetic exchange coupling constants with the broken-symmetry approach,^[25–27] E_{BS} may be regarded as an approximation of the energy of the lowest spin state. They consider that local functionals overestimate the relative stabilization of the lowest spin state relative to the highest spin state.^[28] DFT will usually give larger J values than experimental ones.^[29] Ruiz and co-workers^[26] put forward Equation (10) to calculate J .

$$2J = \frac{E_{\text{BS}} - E_{\text{HS}}}{2S_1S_2 + S_2} \quad (10)$$

However, this formula corresponds strictly to the limit of complete overlap between the magnetic orbitals, and such a hypothesis is not sustained especially for ferromagnetic systems,^[30–31] although it can sometimes give results for J that agree well with experimental values.^[25–27]

Next, we discuss the more rigorous second approach. If one neglects spin-orbit coupling effects, the Hamiltonian for a general extended structure is indicated in Equation (11).

$$\hat{H} = \sum_{i>j} -2J_{ij} \hat{S}_i \cdot \hat{S}_j \quad (11)$$

where \hat{S}_i and \hat{S}_j are the spin operators for the different paramagnetic centers, and the J_{ij} values are the coupling constants between all the paramagnetic centers. Here, we only consider the exchange interactions between nearest neighbors. This fact, together with the

presence of additional symmetry elements in the structure, normally results in a reduced set of J_{ij} values.

There are two pairwise nearest-neighbor MoNi interactions for **A** and four MoNi interactions for **B** (Figure 1 and Figure 3). According to the symmetry, there is one independent coupling constant for **A** [see Equation (12)].

$$J = J_{\text{Mo}(1)\text{Ni}(1)} = J_{\text{Mo}(2)\text{Ni}(1)} \quad (12)$$

There are two independent constants for **B** [Equations (13) and (14)].

$$J = J_{\text{Mo}(1)\text{Ni}(1)} = J_{\text{Mo}(2)\text{Ni}(1)} \quad (13)$$

$$J' = J_{\text{Mo}(1)\text{Ni}(2)} = J_{\text{Mo}(2)\text{Ni}(3)} \quad (14)$$

For **A**² or **B**^{2a}, which have three magnetic centers, the magnetic coupling constants, J , between each nearest-neighbor MoNi pair are the same for the symmetry of the complete structure. Thus, J can be extracted by calculating the energies of two spin states: state 1 with $S = 4$ (all spins up) for **A**² and **B**^{2a} and state 2 with $S = 2$ (Ni atom with spin down) for **A**² and **B**^{2a}. Equation (15) can be used to extract J values.

$$J = (E_2 - E_1)/14 \quad (15)$$

For **B**^{2b}, including state 1 with $S = 7/2$ (all spins up) and state 2 with $S = 1/2$ (Mo atom with spin down), Equation (16) can be used to extract J' values.

$$J' = (E_2 - E_1)/15 \quad (16)$$

To obtain the nearest-neighbor constants, J and J' , for the modeled structures **B**³, we should calculate the energies of three spin states: state 1 with $S = 5$ (all spins up), state 2 with $S = 1$ (all Ni atoms with spins down), and state 3 with $S = 0$ [Ni(1) and one Mo with spins down]. Equations (17) and (18) can be used to extract J and J' values for **B**³.

$$J = (E_3 - E_1)/8 \quad (17)$$

$$J' = (E_2 - E_3)/8 - J \quad (18)$$

For model **B**⁴, the three spin states are as follows: state 1 with $S = 6$ (all spins up), state 2 with $S = 0$ (all Ni atoms with spins down), and state 3 with $S = 4$ [only Ni(2) with spin down]. Equations (19) and (20) can be used to extract J and J' values for **B**⁴.

$$J = (E_3 - E_1)/16 \quad (19)$$

$$J' = (E_2 - E_3)/16 \quad (20)$$

DFT calculations have been performed by using the Amsterdam Density Functional (ADF, version 2005.01b^[32]) package for four models. Illas and co-workers^[33] showed the strong dependence of the calculated J value on the exchange-correlation functionals chosen. Several exchange-correlation functionals were used to evaluate J values. In the calculations of J by using the ADF, the local density approximation (LDA) made use of the Vosko, Wilk, and Nusair^[34] (VWN) local correlation functional. A series of generalized gradient approximations (GGAs), Perdew–Wang 1991 (PW91),^[35] Perdew–Burke–Ernzerhof (PBE)^[36], and the recently developed OPTX–Perdew (OPerded)^[37,38] and OPTX–Perdew–Burke–Ernzerhof (OPBE)^[36,38] functionals were examined. For Mo, Y, Ni, and Zn, the basis set TZV2P (a basis set of triple- ξ quality^[39]) with two

polarization functions) was applied. The basis set DZP (a basis set of double- ξ quality^[39]) supplemented with one polarization function) was used for the other atoms (C, N, O, and H). The inner-core shells of C(1s), N(1s), Zn(1s, 2s, 2p), Y(1s, 2s, 2p, 3s, 3p, 3d), Ni(1s, 2s, 2p), and Mo(1s, 2s, 2p, 3s, 3p, 3d) were treated by the frozen core approximation. The accuracy parameter (accint) for the numerical integration grid was set to 4.0 for all of the complexes. The convergence standard of the system energy was set to be smaller than 10^{-6} eV, which allowed us to reach a precision required for the evaluation of J .

Acknowledgments

This project is supported by the National Natural Science Foundation for the Youth of China (Grant No. 10704041), the Natural Science Foundation of the Jiangsu Higher Education Institutions of China (Grant Nos. 05KJB150055; 07KJB140054), and the Breed Project of Excellent Graduate Degree Thesis of Jiangsu Province of China (Grant No. CX07B_103z).

- [1] a) R. Sessoli, D. Gatteschi, A. Caneschi, M. A. Novak, *Nature* **1993**, *365*, 141–143; b) D. Gatteschi, A. Caneschi, L. Pardi, R. Sessoli, *Science* **1994**, *265*, 1054–1058; c) K. Awaga, Y. Suzuki, H. Hachisuka, K. Takeda, *J. Mater. Chem.* **2006**, *16*, 2516–2521.
- [2] L. Thomas, F. Lioni, R. Ballou, D. Gatteschi, R. Sessoli, B. Barbara, *Nature* **1996**, *383*, 145–147.
- [3] a) H. J. Choi, J. J. Sokol, J. R. Long, *J. Phys. Chem. Solids* **2004**, *65*, 839–844; b) X. Shen, B. Li, J. Zou, Z. Xu, *Trans. Met. Chem.* **2002**, *27*, 372–376; c) H. J. Choi, J. J. Sokol, J. R. Long, *Inorg. Chem.* **2004**, *43*, 1606–1608; d) P. A. Berseth, J. J. Sokol, M. P. Shores, J. L. Heinrich, J. R. Long, *J. Am. Chem. Soc.* **2000**, *122*, 9655–9662.
- [4] a) V. Marvaud, J. M. Herrera, T. Barilero, F. Tuyeras, R. Garde, A. Scullier, C. Decroix, M. Cantuel, C. Desplanches, *Monatsh. Chem.* **2003**, *134*, 149–163; b) V. Marvaud, C. Decroix, A. Scullier, F. Tuyeras, C. Guyard-Duhayon, J. Vaissermann, J. Marrot, F. Gonnet, M. Verdaguer, *Chem. Eur. J.* **2003**, *9*, 1692–1705; c) V. Marvaud, C. Decroix, A. Scullier, C. Guyard-Duhayon, J. Vaissermann, J. Marrot, F. Gonnet, M. Verdaguer, *Chem. Eur. J.* **2003**, *9*, 1677–1691.
- [5] M. P. Shores, J. J. Sokol, J. R. Long, *J. Am. Chem. Soc.* **2002**, *124*, 2279–2292.
- [6] O. Kahn, B. J. Briat, *J. Chem. Soc. Faraday Trans.* **1976**, *72*, 268–281.
- [7] J. J. Girerd, Y. Journaux, O. Kahn, *Chem. Phys. Lett.* **1981**, *82*, 534–538.
- [8] Y. Q. Zhang, C. L. Luo, *J. Phys. Chem. A* **2006**, *110*, 5096–5101.
- [9] Y. Q. Zhang, C. L. Luo, *Eur. J. Inorg. Chem.* **2006**, 2292–2298.
- [10] Y. Q. Zhang, C. L. Luo, *J. Mater. Chem.* **2006**, *16*, 4657–4664.
- [11] Y. Q. Zhang, C. L. Luo, *Eur. J. Inorg. Chem.* **2007**, 1261–1267.
- [12] F. Fabrizi de Biani, E. Ruiz, J. Cano, J. J. Novoa, S. Alvarez, *Inorg. Chem.* **2000**, *39*, 3221–3229.
- [13] C. Blanchet-Boiteux, J. M. Mouesca, *Theor. Chem. Acc.* **2000**, *104*, 257–264.
- [14] C. Desplanches, E. Ruiz, A. Rodríguez-Fortea, *J. Am. Chem. Soc.* **2002**, *124*, 5197–5205.
- [15] T. Cauchy, E. Ruiz, S. Alvarez, *J. Am. Chem. Soc.* **2006**, *128*, 15722–15727.
- [16] A. Szabo, N. S. Ostlund, *Modern Quantum Chemistry*, McGraw-Hill, New York, **1989**.
- [17] E. Ruiz, J. Cano, S. Alvarez, A. Caneschi, D. Gatteschi, *J. Am. Chem. Soc.* **2003**, *125*, 6791–6794.
- [18] E. Ruiz, A. Rodríguez-Fortea, P. Alemany, S. Alvarez, *Polyhedron* **2001**, *20*, 1323–1327.

- [19] E. Ruiz, M. Llunell, P. Alemany, *J. Solid State Chem.* **2003**, *176*, 400–411.
- [20] E. Ruiz, A. Rodríguez-Forteza, J. Cano, S. Alvarez, P. Alemany, *J. Comput. Chem.* **2003**, *24*, 982–989.
- [21] O. Kahn, *Molecular Magnetism*, VCH, New York, **1993**, pp. 211–236.
- [22] L. Noodleman, *J. Chem. Phys.* **1981**, *74*, 5737–5743.
- [23] L. Noodleman, E. J. Baerends, *J. Am. Chem. Soc.* **1984**, *106*, 2316–2327.
- [24] L. Noodleman, D. A. Case, *Adv. Inorg. Chem.* **1992**, *38*, 423–432.
- [25] E. Ruiz, P. Alemany, S. Alvarez, J. Cano, *Inorg. Chem.* **1997**, *36*, 3683–3688.
- [26] E. Ruiz, J. Cano, S. Alvarez, P. Alemany, *J. Comput. Chem.* **1999**, *20*, 1391–1400.
- [27] A. Rodríguez-Forteza, P. Alemany, S. Alvarez, E. Ruiz, *Chem. Eur. J.* **2001**, *7*, 627–637.
- [28] G. L. Gutsev, T. Ziegler, *J. Phys. Chem.* **1991**, *95*, 7220–7228.
- [29] L. Noodleman, D. A. Case, A. Aizman, *J. Am. Chem. Soc.* **1988**, *110*, 1001–1005.
- [30] J. M. Mouesca, J. L. Chen, L. Noodleman, D. Bashford, D. A. Case, *J. Am. Chem. Soc.* **1994**, *116*, 11898–11914.
- [31] I. Rudra, Q. Wu, T. V. Voorhis, *J. Chem. Phys.* **2006**, *124*, 024103 (1–9).
- [32] a) G. te Velde, F. M. Bickelhaupt, E. J. Baerends, C. Fonseca Guerra, S. J. A. van Gisbergen, J. G. Snijders, T. Ziegler, *J. Comput. Chem.* **2001**, *22*, 931–967; b) C. Fonseca Guerra, G. J. G. Snijders, G. te Velde, E. J. Baerends, *Theor. Chem. Acc.* **1998**, *99*, 391–403; c) ADF2005.01b, SCM, Theoretical Chemistry, Vrije Universiteit, Amsterdam, The Netherlands, <http://www.scm.com>.
- [33] F. Illas, I. de P. R. Moreira, J. M. Bofill, M. Filatov, *Phys. Rev. B* **2004**, *70*, 132414 (1–4).
- [34] S. H. Vosko, L. Wilk, M. Nusair, *Can. J. Phys.* **1980**, *58*, 1200–1211.
- [35] J. P. Perdew, J. A. Chevary, S. H. Vosko, K. A. Jackson, M. R. Pederson, D. J. Singh, C. Fiolhais, *Phys. Rev. B* **1992**, *46*, 6671–6687.
- [36] J. P. Perdew, K. Burke, M. Ernzerhof, *Phys. Rev. Lett.* **1996**, *77*, 3865–3868.
- [37] N. C. Handy, A. J. Cohen, *Mol. Phys.* **2001**, *99*, 403–412.
- [38] J. P. Perdew, *Phys. Rev. B* **1986**, *33*, 8822–8824.
- [39] A. Schaefer, C. Huber, R. Ahlrichs, *J. Chem. Phys.* **1994**, *100*, 5829–5835.

Received: January 8, 2008

Published Online: March 19, 2008